Improvement of Torque Control for an Assistant Electric Power Steering System using a Type-2 Fuzzy Logic Controller

Vo Thanh Ha
Faculty of Electrical and Electronic Engineering, University of Transport and Communications, Vietnam
vothanhha.ktd@utc.edu.vn (corresponding author)

Received: 15 April 2024 | Revised: 7 May 2024 | Accepted: 10 May 2024

 DOI: https://doi.org/10.48084/etasr.7494

ABSTRACT

This article explains how a type 2 fuzzy logic controller can improve the torque of a 3-phase Permanent Magnet Synchronous Motor (PMSM) in an electric power steering system. The goal is to ensure effective electric power steering under various road conditions and speeds. The implementation of type-2 Type-2 Fuzzy Logic Controller (FLC) involves fuzzification, inference, and output processing. Type-reduction methods are more advanced than type-1 defuzzification methods, handling more rule uncertainties. While computationally demanding, a simple type-reduction computation process is outlined for interval type-2 fuzzy sets. The type 2 fuzzy logic controller algorithm manages the PMSM motor using Field-Oriented Control (FOC), adjusting the motor voltage based on torque, speed, and steering angle sensor inputs. The study's results provide a solid basis for future research on designing and controlling electric power steering systems with precision and efficiency. This research sets the stage for improved electric power steering systems, contributing to the development of intelligent automotive technologies.

Keywords-EPS; type-2 FLC; FOC; PMSM

I. INTRODUCTION

The steering mechanism of cars has been continuously improving to meet safety and comfort requirements, particularly for high-speed driving and challenging situations such as heavy traffic [1]. Introducing the Electric Power Steering (EPS) system marked a significant breakthrough in automobile technology. The EPS system provides electrical power to the steering mechanism, enabling the driver to quickly and effectively control the vehicle's direction. This technology enhances the capacity of cars to change direction and move smoothly, guaranteeing the comfort and safety of drivers [2]. In addition, EPS minimizes fuel consumption, is straightforward to maintain and repair, and provides exceptional performance in comparison with other power steering systems [3]. Determining and managing the electric motor's power steering torque govern the steering system's functioning and operational needs, which in turn impact the safety of the vehicle's motion. To enhance the driving experience and improve safety, it is recommended that power steering is able to adapt to both the speed of the car and the amount of the steering force used by the driver [4, 5]. The EPS model in [6, 7] is formulated deploying mathematical equations, whereas the mechanical subsystem of the steering unit is designed based on the dynamic equations of the steering unit. The entire mathematical model of EPS employing PMSM was developed in MATLAB/Simulink and evaluated on the Embedded Controller NI PXI-e 8135 processor. Various scenarios were implemented using NI Verstand. Furthermore, improving steering feel usually entails examining the steering system and electric power steering logic, suggesting a technique for determining relevant parameters for steering feel, and adjusting the electric power steering control system to attain the desired steering characteristics [8]. Authors in [9] proposed a method that utilizes the mathematical model of the system's steering torque to enhance the steering sensation. This model engages parameters obtained from the steering system data. A method for torque compensation was proposed and confirmed via trials to improve the steering experience for drivers. Authors in [10] described a control technique that actively addresses friction in a CEPS system. This strategy involves employing the assist motor and electronic control unit to mitigate the adverse effects of friction and imitate an ideal system without friction. More recently, the development of several approaches for designing EPS controllers has resulted in many tactics to improve the steering feel and torque response. These strategies encompass the utilization of control algorithms for linear systems, such as PI, PID [11], fuzzy [12], wavelet fuzzy neural networks [13], genetic fuzzy [14], fuzzy neural sliding-mode [15], and an LQG integration of the backstepping (BS) method with PID control [16]. It has been highlighted [17] that these control strategies exhibit remarkable efficacy in some circumstances despite certain unresolved technical obstacles.

This article elucidates how a type 2 fuzzy logic controller might enhance the torque output of a 3-phase Permanent Magnet Synchronous Motor (PMSM) inside an electric power steering system. The objective is to provide efficient electric

power steering across different road conditions and velocities. Type-2 Fuzzy Logic Controller (FLC) system implementation comprises fuzzification, inference, and output processing. Type-reduction approaches are superior to type-1 defuzzification methods since they can effectively manage a greater degree of rule uncertainty.

II. MATHEMATICAL DESCRIPTION OFTHE EPS DYNAMIC MODEL AND PMSM

While designing the model for a car's power steering system putting into service a PMSM motor, it is crucial to consider some fundamental assumptions. Firstly, the model assumes that the PMSM exhibits symmetry to streamline the design process. The precision of the model depends on the effective operation of sensors and control systems. Furthermore, it is essential to consider humidity and temperature to guarantee the model's accuracy under all working situations. These assumptions optimize the model and facilitate designing and using the control system. The simulation integrates the EPS simulation parameters outlined in Table I with the PMSM simulation parameters specified in Table II.

TABLE I. THE EPS PARAMETERS

Parameters	Symbol	Value	Unit
The inertia of the steering wheel and steering shaft	J_s	0.0012	[kg.m^2]
The friction coefficient of the steering shaft	B_s	0.26	[Nm.rad^{-1}s]
Torsional stiffness of the steering shaft	K_s	115	[Nm. rad^{-1}]
Torsional stiffness of motor shaft and gear box	K_m	125	[Nm. rad^{-1}]
Transmission ratio of the gear box	i_m	7.225	
Resistance coefficient between gear and rack	B_r	653.203	[Nsm^{-1}]
Mass of the gear and rack	m	32	[kg]
Linear stiffness	K_r	91061.4	[N/m]
Gear radius	r_p	0.007783	[m]

TABLE II. THE PMSM MOTOR PARAMETERS

Parameters	Symbol	Value	Unit
Stator resistor	R_s	0.1	[Ω]
Stator coil inductance	L_s	0,1	[mH]
Number of pole pairs	p_n	4	
Flux link	φ_f	0,0175	[Wb]
Moment of inertia of the motor	J_m	0,0004704	[kgm^2]
The friction coefficient of the motor	B_m	0,003339	[Nm.rad^{-1}s]

A. The EPS Dynamic Model

The equation that represents the relationship between the steering wheel and the steering column is:

$$J_s\ddot{\theta}_s = T_d - K_s(\theta_s - \theta_r) - B_s\dot{\theta}_s \quad (1)$$

The following equation defines the assistance section:

$$J_m\ddot{\theta}_m = T_m - K_m(\theta_m - i_m\theta_r) - B_m\dot{\theta}_m \quad (2)$$

The equation in the section of rack and pinion is:

$$m\ddot{\theta}_x = \frac{1}{r_p}[K_m(\theta_m - i_m\theta_r)i_m + K_s(\theta_s - \theta_r)] - B_r\dot{x} - K_r x \quad (3)$$

where T_d and T_m are the steering wheel's input torque and the motor's output torque separately, θ_s, θ_r, and θ_m are the turn angles of the steering wheel, steering column, and motor, and x is the displacement of the rack.

Using (1) and (3), the EPS mechanism component model is constructed in MATLAB (Figures 1-2).

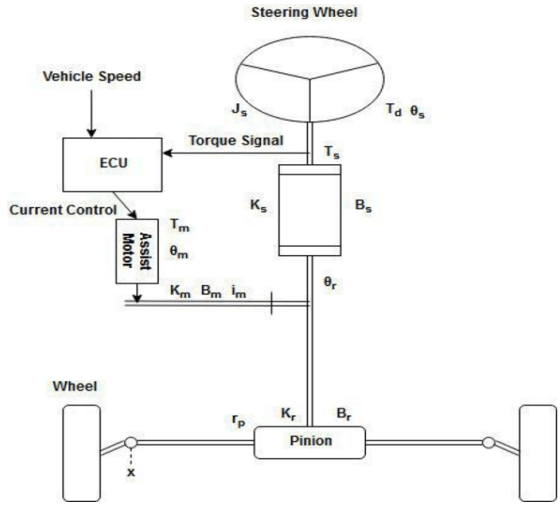

Fig. 1. The EPS mechanism component.

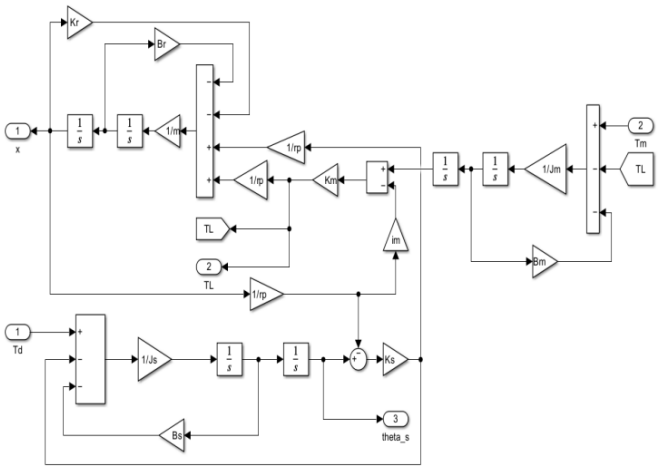

Fig. 2. Simulation of the EPS mechanism component.

B. Mathematical Model of the PMSM

In order to build the PMSM model, this study disregards the saturation of the motor's iron core and the leakage flux. To ensure uniform distribution of the air gap between the stator and rotor and to certify that the magnetic circuit is not affected by the location of the rotor (meaning that the inductance of each coil is not dependent on the rotor), specific measures need to be taken. The stator voltage vector equation is as written:

$$U_s = R_s i_s + L_s \dot{i_s} + \dot{\varphi}_s e^{j\theta_r} \quad (4)$$

where $U_s, R_s, i_s, L_s, \varphi_s$ are the voltage of stator terminal, the resistance of stator winding, stator current, stator inductance and coupling magnetic linkage of the rotor magnet on the stator side.

The voltage equation on the *dq* coordinate system is:

$$\begin{cases} u_{sd} = R_s i_{sd} + \dot{\varphi}_{rd} - \omega_r \varphi_{sq} \\ u_{sq} = R_s i_{sq} + \dot{\varphi}_{rq} + \omega_r \varphi_{sd} \\ \varphi_{sd} = L_{sd} i_{sd} + \varphi_f \\ \varphi_{sq} = L_{sq} i_{sq} \end{cases} \quad (5)$$

The electromagnetic torque of the PMSM in the *dq* axis is:

$$T_m = p_n(\varphi_{rd} i_{sq} - \varphi_{rq} i_{sd}) = p_n[\varphi_f i_{sq} + (L_{sd} - L_{sq}) i_{sd} i_{sq}] \quad (6)$$

The equation of motor motion is:

$$\dot{\omega}_r = T_m - T_L - B_m \omega_r \quad (7)$$

where: $u_{sd}, u_{sq}, i_{sd}, i_{sq}, \varphi_{rd}, \varphi_{rq}, L_{sd}, L_{sq}$ are the stator winding voltage, current, magnetic linkage and inductance in the *dq* axis, φ_f is the rotor magnetic linkage, p_n is the number of motor pole-pairs, ω_r is the motor's angular frequency, and T_L is the load torque.

C. Model of EPS Characteristic

The EPS characteristic curve shows how the input signal (steering torque and vehicle speed) relates to the output signal (steering torque or current to the electric power steering motor). When driving, the force on the steering wheel decreases as the vehicle's speed increases, causing the electric motor's force on the steering wheel to decrease. Creating this curve involves using specific parameters obtained from real-world tests and experiments. Equation (8) describes how the electric motor can produce the proper torque based on the torque sensor signal and motor speed.

$$T_M = \begin{cases} 0, & 0 \le T_d \le T_{d0} \\ trq(v), & T_{d0} < T_d < T_{dmax} \\ T_{Mmax}, & T_d \ge T_{dmax} \end{cases} \quad (8)$$

where:

$$trq(v) = (4 - 0.0606V + 0.0003V^2)(T_d - T_{d0}) \quad (9)$$

This formula determines steering assistance for EPS, ensuring smooth steering in diverse driving conditions. Engineers adjust the variables to enhance efficiency and user experience. Table III portrays the power steering torque at different speeds with max steering wheel torque, T_{dmax}. Utilizing the values from Table I, we can create the power steering curve in Figure 3.

TABLE III. POWER STEERING TORQUE AT DIFFERENT SPEEDS WITH MAX STEERING WHEEL TORQUE

Velocity (km/h)	Torque T_{Mmax} (Nm)
0	24
30	20.71
60	17.8
90	15.7
120	13.9

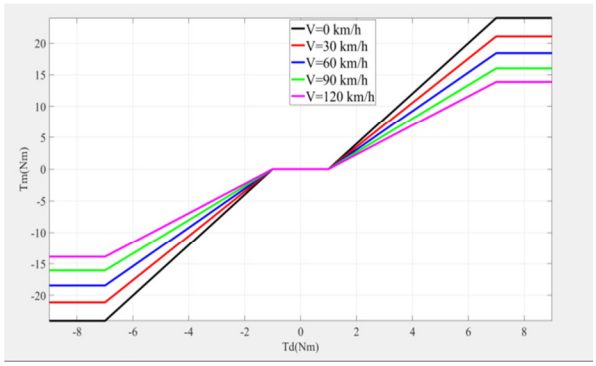

Fig. 3. The power steering characteristic curve.

In this specific scenario T_M is the required torque of the electric motor that must be transmitted after passing through the gear reduction box, T_{d0} represents the minimum steering wheel torque needed to activate the electric motor for power steering ($T_{d0} = 1$ Nm),and T_{dmax} is the maximum steering wheel torque the driver exerts. At this point, the electric motor reaches its full capability. Choosing a value for T_{dmax} based on experience is recommended, with a suggested value of 7 Nm. When the torque exceeds 7 Nm, the motor consistently gives a steady torque. If the input torque T_d is below the threshold value T_{d0}, the electric motor will not provide power for adequate steering responsiveness at low steering angles. When the electric motor's torque demand T_d falls between T_{d0} and T_{dmax}, the motor torque T_M will increase linearly in response to T_d. The coefficient $trq(v)$ will vary inversely with the vehicle speed. If T_d exceeds the maximum threshold T_{dmax}, the electric motor will consistently deliver maximum torque. As the vehicle speed increases, the torque assistance from the electric motor decreases gradually. When the car is stationary, the motor produces the maximum current, I_{max}, for optimal maneuverability during local turns. If the input torque of the steering wheel, T_d, is below the threshold value T_{d0}, and T_d is greater than or equal to T_{dmax}, (1 Nm), the engine will not provide power. The motor will consistently give a steady torque when the torque exceeds 7 Nm.

III. INTERVAL TYPE-2 FUZZY CONTROLLER

The structure of Type-2 fuzzy is depicted in Figure 4.

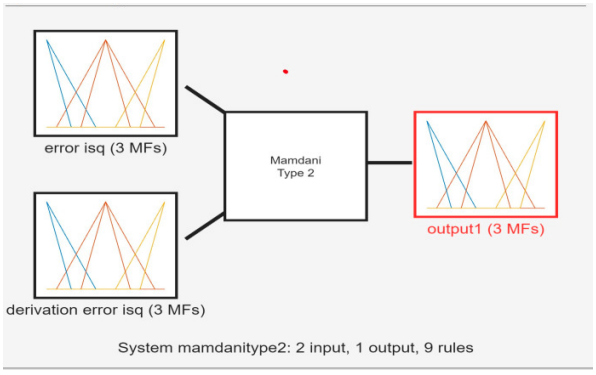

Fig. 4. The structure of type-2 FLC.

Figure 4 indicates that the adaptive FLC scheme consists of four layers: layer 1 (input) and layer 2 (fuzzification) form the antecedent part of the fuzzy rules. The weight matrix W links layer 3 (fuzzy rules) and layer 4 (output) to establish the adaptive fuzzy logic consequent element. Due to the substantial uncertainty, higher kinds of fuzzy sets must be examined in particular situations. Type-2 fuzzy engines are well-suited for time-variant systems with uncertain and changing dynamics throughout time. Nevertheless, the computational cost of operations on fuzzy sets escalates as the fuzzy set's nature rises. Interval type-2 fuzzy systems, known for their simplicity and efficiency, may be used to reduce the inherent computing complexity. Type-2 FLC comprises a fuzzifier, a rule base, a fuzzy inference engine, a type reducer, and a denitrifier. The type-reduced set generates the leftmost and rightmost points, denoted as y_{tk} and y_{pr}, respectively. The set is defuzzified by calculating the average value of the interval set to provide a precise output value. The defuzzified output for each output k is stated as [19-21]:

$$Y_k(x) = \frac{y_{tk}+y_{pk}}{2} \quad (10)$$

Conversely, the established regulations are designed to ensure that both the error in the machine's stator currents (i_{sq}) and its derivative approach zero, based on the following three principles: (1) When both error signals deviate significantly from their respective nominal zero-valued surfaces, the output of the FLC increases, (2) as the errors approach the nominal zero-valued surfaces, the output is gradually adjusted to a smaller value to ensure a smoother approach, (3) once the error reaches the nominal zero-valued surface, the output is set to zero. System mandanity type 2-fuzzy logic is considered, which has 2 inputs and 01 output with 9 rules.

Figures 5-7 show the input membership functions, while Figure 8 presents the fuzzy rules. The individuals were selected based on their excellent performance, as determined via empirical analysis. These individuals may be further modified to enhance control performance. Defuzzification is accomplished adopting the center-of-area approach.

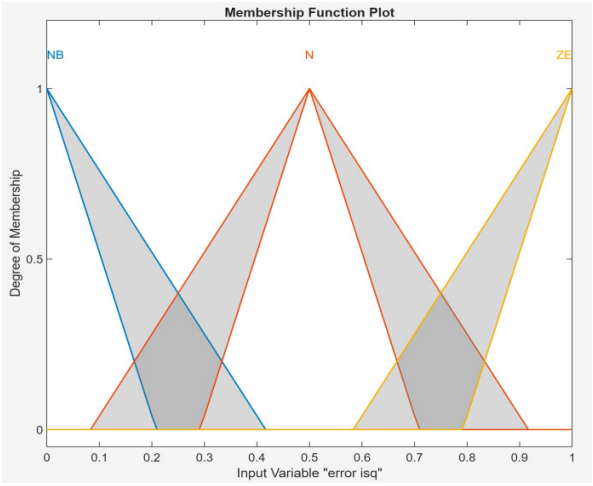

Fig. 5. Input 1 for system mandanity type 2-FLC.

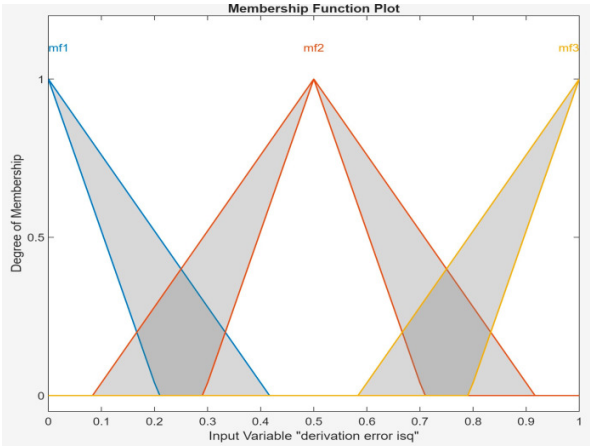

Fig. 6. Input 2 for system mandanity type 2-FLC.

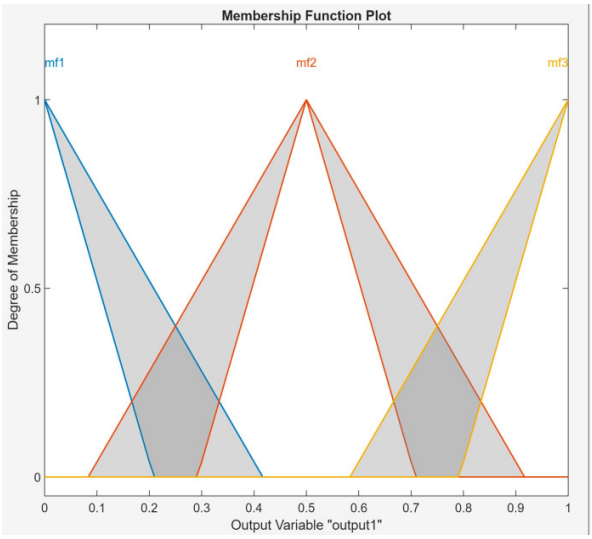

Fig. 7. Output for system mandanity type 2-FLC.

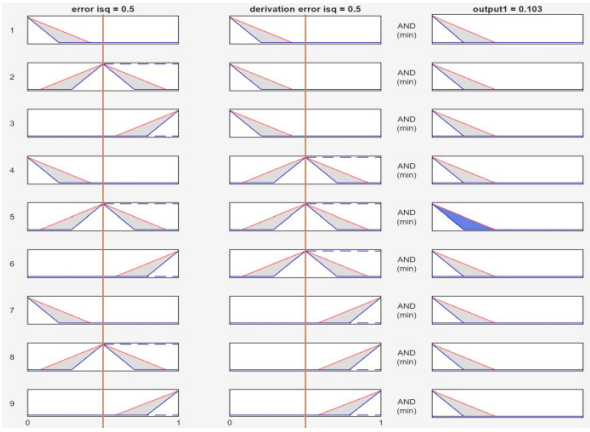

Fig. 8. The fuzzy rules.

IV. SIMULATION RESULTS AND ANALYSIS

Figure 9 discloses the layout of the EPS control simulation for cars.

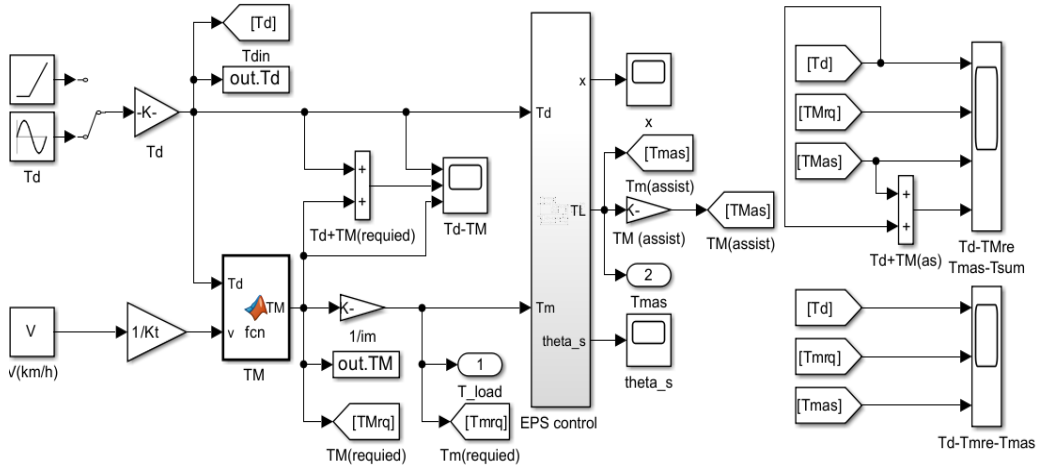

Fig. 9. The EPS control simulation structure.

The simulation was conducted in MATLAB/Simulink and involved steering torque inputs in the form of sine signals. The first simulation tested sinusoidal variations in steering wheel torque and assist features for 10 s under static and steering conditions. With a steering wheel input torque of 9 Nm and an angular frequency of π/3, different speed levels of 0 km/h, 30 km/h, 60 km/h, 90 km/h, and 120 km/h were analyzed.

The steering wheel input torque response, denoted as T_d, is a sinusoidal signal that varies with the vehicle speed V. The torque response is influenced by the supporting torque T_M (assistance), the needed torque T_M^* (required), and the total torque T_{sum}, as observed in Figures 11, 13, 15, 17, and 19. The present answers, i_d, and i_q, are illustrated in Figures 10, 12, 14, 16, and 18

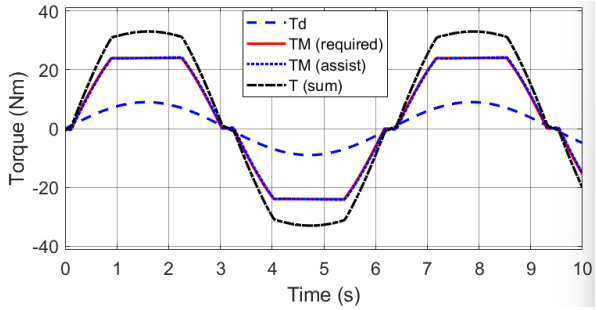

Fig. 10. The torque response when V = 0 km/h.

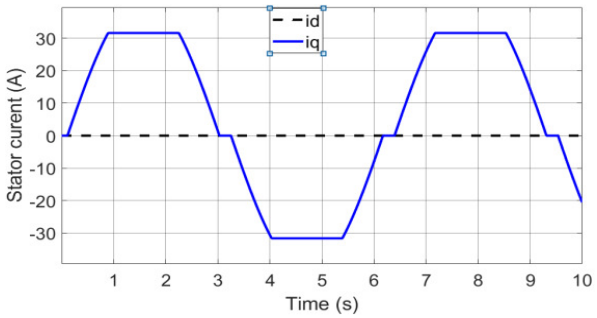

Fig. 11. The stator current when V = 0 km/h.

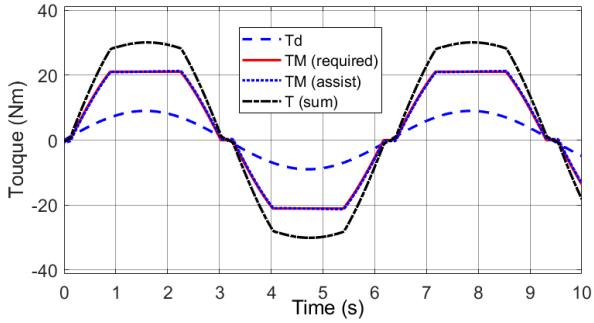

Fig. 12. The torque response when V = 30 km/h.

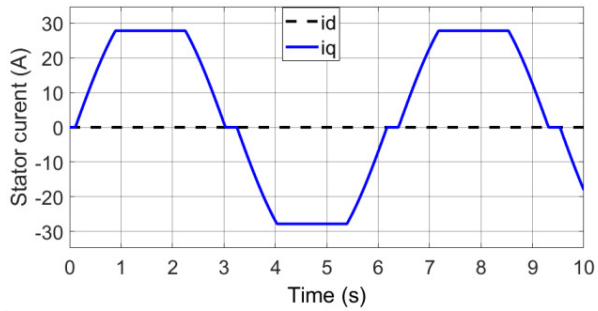

Fig. 13. The stator current when V = 30 km/h.

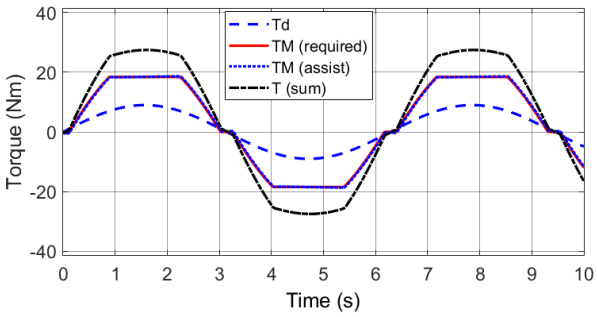

Fig. 14. The torque response when V = 60 km/h.

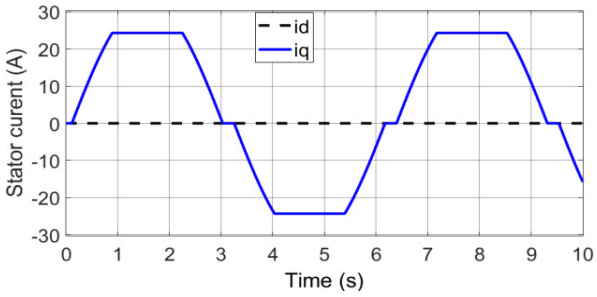

Fig. 15. The stator current when V = 60 km/h.

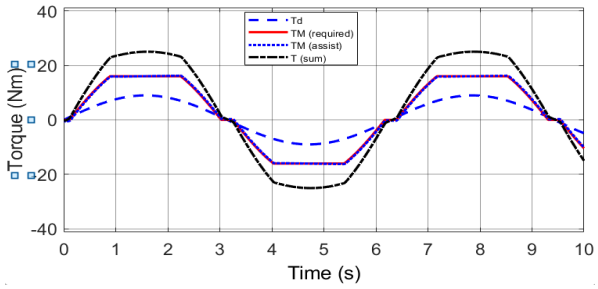

Fig. 16. The torque response when V = 90 km/h.

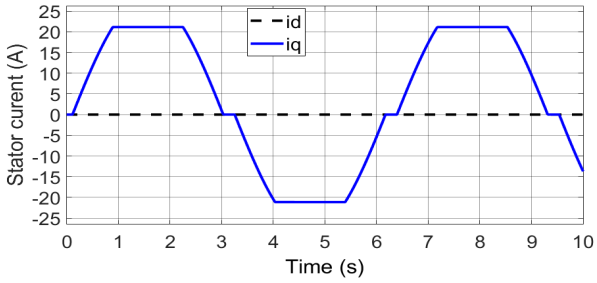

Fig. 17. The stator current when V = 90 km/h.

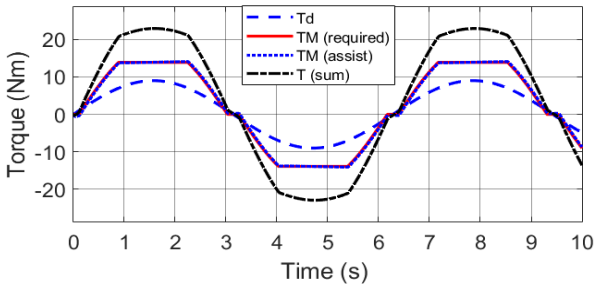

Fig. 18. The torque response when V = 120 km/h.

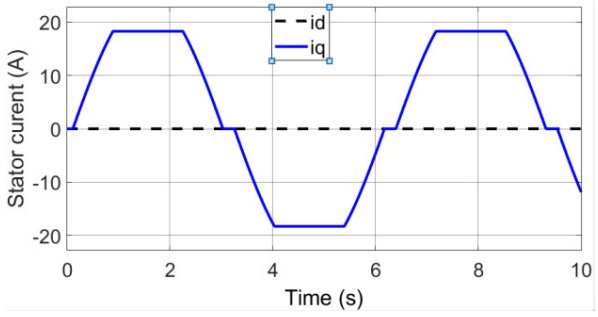

Fig. 19. The stator current when V = 120 km/h.

The Figures exhibit that the EPS unit effectively meets the desired torque support requirements by adjusting the power steering torque based on the steering torque signal and vehicle speed, as described in Figures 10, 12, 14, 16, and 18. The electric motor's supporting torque closely matches the required torque with slight variation, demonstrating the accuracy and effectiveness of the type -2 FLC using the FOC control algorithm. Additionally, the system's response time to changes in steering torque and vehicle speed is remarkably quick, ensuring a seamless driving experience for the user. The integration of the type -2 FLC with FOC control showcases a sophisticated level of control and precision in managing the power steering assistance, leading to enhanced vehicle handling and manoeuvrability. Overall, the results highlight the advanced capabilities and performance of the EPS unit in meeting the dynamic requirements of modern automotive systems. When the torque is 1 Nm or less, the current and torque motor are 0, keeping the power steering inactive. The power steering activates when the torque exceeds 1 Nm, increasing between 1 to 7 Nm, leading to variable increases in current intensity and power steering torque up to their maximum values. At its peak, the power steering system delivers a seamless driving experience, effortlessly adapting to varying road conditions and enhancing control for the driver. This dynamic interplay of torque, current, and power steering ensures optimal performance and safety, making every journey a smooth and responsive one.

In the simulation results manifested in Figures 11, 13, 15, 17, and 19, it can be seen that once the torque exceeds 7 Nm, both current and torque peak. Even with additional torque increments, these peak values stay consistent. The peak current and torque values exhibit an inverse relationship with vehicle speed, which spans from 0 to 120 km/h. The peak current varies from 31.6 to 18.3 A, whereas the peak torque ranges from 24.0 to 13.9 Nm. This behavior suggests a sophisticated control system that effectively manages the power delivery to the vehicle's drivetrain across a wide range of speeds. The consistent peak values of current and torque, despite additional torque increments, indicate a well-optimized system that ensures stable performance under varying load conditions. The observed inverse relationship between peak current/torque and vehicle speed highlights the dynamic nature of the power distribution, adapting to the driving conditions for optimal efficiency and performance. Such intricate control mechanisms are crucial for achieving a balance between power output, energy consumption, and overall driving experience in electric vehicles. In summary, the rule aligns well with the steering system's characteristics: the steering resistance decreases as the vehicle speed increases. Electric power steering guarantees smooth steering at low speeds and a satisfactory experience at high speeds.

V. CONCLUSIONS

The electric power steering system operates based on a nonlinear state model affected by speed, steering angle, and road surface. This requires a compact drive system, a high-torque motor, and a suitable control method to handle the nonlinear aspects effectively. The study suggests using a type 2 fuzzy logic controller to regulate torque for the PMSM engine,

enhancing torque across various vehicle speeds. Additionally, this approach ameliorates driving stability and safety by decreasing assist torque from 24 Nm to 13.9 Nm between 0 km/h and 120 km/h. The envisioned power steering solution aims to provide smooth steering performance at all speeds, explicitly focusing on analyzing sinusoidal torque signals at varying frequencies.

This project contributes to the existing research results of torque control for electric power steering systems using nonlinear control. The results of this research have overcome the disadvantages of the type 1 fuzzy logic, PID, and LQR controllers. It is a controller that can adapt to nonlinear patterns, environmental disturbances, and different speed ranges. The correctness of the solution was initially demonstrated by MATLAB simulations. To enhance control reliability, integrating torque signals at diverse frequencies is crucial. Moreover, the implementation of this control solution for real-world applications is imminent.

ACKNOWLEDGMENT

This research is funded by the University of Transport and Communications (UTC).

REFERENCES

[1] F. Wilhelm, T. Tamura, R. Fuchs, and P. Müllhaupt, "Friction Compensation Control for Power Steering," *IEEE Transactions on Control Systems Technology*, vol. 24, no. 4, pp. 1354–1367, Jul. 2016, https://doi.org/10.1109/TCST.2015.2483561.

[2] Y.-C. Hung, F.-J. Lin, J.-C. Hwang, J.-K. Chang, and K.-C. Ruan, "Wavelet Fuzzy Neural Network With Asymmetric Membership Function Controller for Electric Power Steering System via Improved Differential Evolution," *IEEE Transactions on Power Electronics*, vol. 30, no. 4, pp. 2350–2362, Apr. 2015, https://doi.org/10.1109/TPEL.2014.2327693.

[3] A. Badawy, J. Zuraski, F. Bolourchi, and A. Chandy, "Modeling and analysis of an electric power steering system," SAE, SAE Technical Paper No. 1999-01-0399, 1999.

[4] W. Kim, Y. S. Son, J. Y. Yu, C. M. Kang, and C. C. Chung, "Torque Overlay Based Robust Steering Wheel Angle Control for Lateral Control Using Backstepping Design," *IFAC Proceedings Volumes*, vol. 47, no. 3, pp. 12035–12041, Jan. 2014, https://doi.org/10.3182/20140824-6-ZA-1003.00803.

[5] M. Ruba, R. Nemes, F. P. Piglesan, H. Hedesiu, and C. Martis, "Complete elecric power steering system real-time model in the loop simulator," in *2018 ELEKTRO*, Mikulov, Czech Republic, Feb. 2018, https://doi.org/10.1109/ELEKTRO.2018.8398354.

[6] R. R. Hiremath and T. B. Isha, "Modelling and simulation of electric power steering system using permanent magnet synchronous motor," *IOP Conference Series: Materials Science and Engineering*, vol. 561, no. 1, Jul. 2019, Art. no. 012124, https://doi.org/10.1088/1757-899X/561/1/012124.

[7] R. G. Krishnan, T. B. Isha, and P. Balakrishnan, "A back-EMF based sensorless speed control of permanent magnet synchronous machine," in *2017 International Conference on Circuit, Power and Computing Technologies (ICCPCT)*, Kollam, India, Apr. 2017, https://doi.org/10.1109/ICCPCT.2017.8074313.

[8] R.-O. Nemes, M. Ruba, and C. Martis, "Integration of Real-Time Electric Power Steering System Matlab/Simulink Model into National Instruments VeriStand Environment," in *2018 IEEE 18th International Power Electronics and Motion Control Conference (PEMC)*, Budapest, Hungary, Dec. 2018, pp. 700–703, https://doi.org/10.1109/EPEPEMC.2018.8521888.

[9] S. Woo, C. Heo, M.-O. Jeong, and J.-M. Lee, "Integral Analysis of a Vehicle and Electric Power Steering Logic for Improving Steering Feel Performance," *Applied Sciences*, vol. 13, no. 20, Jan. 2023, Art. no. 11598, https://doi.org/10.3390/app132011598.

[10] J. H. Choi, K. Nam, and S. Oh, "Steering feel improvement by mathematical modeling of the Electric Power Steering system," *Mechatronics*, vol. 78, Oct. 2021, Art. no. 102629, https://doi.org/10.1016/j.mechatronics.2021.102629.

[11] F. Wilhelm, T. Tamura, R. Fuchs, and P. Müllhaupt, "Friction Compensation Control for Power Steering," *IEEE Transactions on Control Systems Technology*, vol. 24, no. 4, pp. 1354–1367, Jul. 2016, https://doi.org/10.1109/TCST.2015.2483561.

[12] D. Saifia, M. Chadli, H. R. Karimi, and S. Labiod, "Fuzzy control for Electric Power Steering System with assist motor current input constraints," *Journal of the Franklin Institute*, vol. 352, no. 2, pp. 562–576, Feb. 2015, https://doi.org/10.1016/j.jfranklin.2014.05.007.

[13] L. Cai, A. B. Rad, and W.-L. Chan, "A Genetic Fuzzy Controller for Vehicle Automatic Steering Control," *IEEE Transactions on Vehicular Technology*, vol. 56, no. 2, pp. 529–543, Mar. 2007, https://doi.org/10.1109/TVT.2006.889576.

[14] A. Akpunar and S. Iplikci, "Runge-Kutta Model Predictive Speed Control for Permanent Magnet Synchronous Motors," *Energies*, vol. 13, no. 5, Jan. 2020, Art. no. 1216, https://doi.org/10.3390/en13051216.

[15] H. Bassi and Y. A. Mobarak, "State-Space Modeling and Performance Analysis of Variable-Speed Wind Turbine Based on a Model Predictive Control Approach," *Engineering, Technology & Applied Science Research*, vol. 7, no. 2, pp. 1436–1443, Apr. 2017, https://doi.org/10.48084/etasr.1015.

[16] D. T. Tu, "Enhancing Road Holding and Vehicle Comfort for an Active Suspension System utilizing Model Predictive Control and Deep Learning," *Engineering, Technology & Applied Science Research*, vol. 14, no. 1, pp. 12931–12936, Feb. 2024, https://doi.org/10.48084/etasr.6582.

[17] P. Weyers, A. Barth, and A. Kummert, "Driver State Monitoring with Hierarchical Classification," in *2018 21st International Conference on Intelligent Transportation Systems (ITSC)*, Maui, HI, USA, Aug. 2018, pp. 3239–3244, https://doi.org/10.1109/ITSC.2018.8569467.